RAB20 Promotes Proliferation via G2/M Phase Through the Chk1/cdc25c/cdc2-cyclinB1 Pathway in Penile Squamous Cell Carcinoma

Xingliang Tan
Sun Yat-sen University Cancer Center
Gangjun Yuan
Chongqing Medical University
Yanjun Wang
Sun Yat-sen University Cancer Center
Dong Chen
Sun Yat-sen University Cancer Center
Yuantao Zou
Sun Yat-sen University Cancer Center
Sihao Luo
Sun Yat-sen University Cancer Center
Hui Han
Sun Yat-sen University Cancer Center
Zike Qin
Sun Yat-sen University Cancer Center
Zhuowei Liu
Sun Yat-sen University Cancer Center
Fangjian Zhou
Sun Yat-sen University Cancer Center
Yanling Liu
Sun Yat-sen University Cancer Center
Kai Yao (yaokai@sysucc.org.cn)
Sun Yat-sen University Cancer Center https://orcid.org/0000-0002-2589-3058

Research

Keywords: RAB20, penile squamous cell carcinoma, cell proliferation, cell cycle, prognostic biomarker

Posted Date: September 28th, 2021

DOI: https://doi.org/10.21203/rs.3.rs-927245/v1

Version of Record: A version of this preprint was published at Cancers on February 22nd, 2022. See the published version at https://doi.org/10.3390/cancers14051106.

Abstract

Background: RAB20, a member of the RAS GTPase oncogene family, promotes tumorigenesis in several cancers with poor survival outcomes but its role in penile squamous cell carcinoma (PSCC) remains unclear. Here, comprehensive genomic profiling was performed on eight PSCC and normal tissue pairs and revealed that RAB20 is upregulated in tumors, especially in metastatic lymph nodes. We aimed to explore the clinical significance and oncogenic effect of RAB20 on PSCC and to identify its specific mechanisms in tumor progression.

Methods: RT-qPCR and Western blotting were performed on PSCC tissue pairs and our newly established PSCC cell lines to examine the RAB20 expression pattern. The clinical relevance and prognostic value of RAB20 were validated by immunohistochemistry in samples from 259 PSCC patients, the largest cohort to date. Cell proliferation, migration, colony formation, and cell cycle assays were performed along with analysis of a nude mouse tumorigenesis model to explore RAB20's oncogenic functions. RAB20-mediated G2/M phase cell cycle arrest mechanisms were further demonstrated by bioinformatics analysis and Western blotting.

Results: RAB20 expression was upregulated in PSCC tissues, especially in metastatic lymph nodes. High RAB20 expression in PSCC was associated with T, N, and M status, extranodal extension and clinical stage ($P < 0.01$). Survival analysis indicated that RAB20 was an unfavorable independent prognostic indicator ($p = 0.011$, HR = 2.090; 95% CI: 1.183–4.692), and patients with high expression experienced shorter 5-year cancer-specific survival ($P < 0.001$). Furthermore, knockdown of RAB20 inhibited cell growth and tumorigenesis *in vitro* and *in vivo.* Mechanistic studies indicated that RAB20 depletion arrested the PSCC cell cycle at G2/M via the Chk1/cdc25c/cdc2-cyclinB1 pathway.

Conclusions: RAB20 promotes PSCC progression, predicting advanced disease with poor outcomes. RAB20 could be a promising prognostic biomarker and potential therapeutic target for PSCC.

Background

Penile squamous cell carcinoma (PSCC), with a global incidence of 0.4–0.6/100000, is a devastating genitourinary disease in males [1, 2]. Compared with the histologic features and pathologic stages of the primary tumor, lymph node metastasis is the most unfavorable factor affecting long-term survival outcomes, and PSCC patients have a dismal 5-year cancer-specific survival rate (CSS) of approximately 29–59% [3–6]. Currently, researchers face significant challenges and difficulties in investigating the progression and invasion of PSCC owing to the tumor heterogeneity [4, 7, 8]. Although several genomic studies have revealed that EGFR amplifications and CDKN2A mutations are frequent somatic alterations in metastatic PSCC, their clinical significance and expression profiles during tumor progression remain elusive owing to noncomprehensive transcriptome sequencing methods, small sample sizes and unpaired PSCC tissues [8–10]. Overexpression of BIRC5 [11], IDO1 [12] and LAMC2 [13] was found to be associated with advanced disease and poor prognosis, enhancing PSCC cell proliferation and invasion,

but the detailed mechanism of tumor progression remains unclear. Despite research progress, the lack of appropriate cell lines and large-scale clinical validation methods greatly hinders the exploration of biomarkers associated with the PSCC progression.

To identify potential prognostic markers of PSCC and intrinsic mechanisms, eight pairs of pN + PSCC tissues (normal tissues, primary tumor and metastatic lymph node) were subjected to whole-transcriptome comprehensive genomic profiling. We found that RAB20 was the critical oncogene overexpressed in PSCC tissues, especially in metastatic lymph nodes, and was associated with poor survival. However, the roles of RAB20 and its specific mechanisms in PSCC are still unknown.

RAB20 belongs to the Rab family of small GTPases, which plays a critical role in membrane trafficking in epithelial cells and has been found to be associated with the progression of several cancers [14]. Overexpression and amplification of RAB20 has been detected in pancreatic carcinoma, colorectal adenoma and triple-negative breast cancer and is associated with high-risk clinicopathological stages and poor survival outcomes [15–17].

In this study, we investigated the expression pattern of RAB20 in PSCC tissues and demonstrated a correlation between RAB20 expression and clinicopathological features in 259 PSCC patients, the largest cohort reported to date. We identified that RAB20 is an independent prognostic indicator correlated with poor survival outcomes. Furthermore, by using newly established PSCC cell lines and animal models [18], we demonstrated that RAB20 promotes cell proliferation and tumor progression, inducing G2/M phase cell cycle arrest via the Chk1/cdc25c/cdc2-cyclinB1 pathway.

Methods

Patient cohort, samples and research ethics

This study included a total of 259 patients who were diagnosed with pathologically confirmed PSCC at the Sun Yat-sen University Cancer Center (SYSUCC) between January 2000 and December 2019. For each patient, their clinical, pathological and survival information was retrospectively reviewed according to the TNM Staging System for Penile Cancer (8th ed., 2017). For human tissue samples, 8 pairs of pN + PSCC matched tissues were retrieved for comprehensive genomic profiling (CGP). Ninety-nine fresh frozen samples (78 tumor tissues and 21 normal tissues) were collected for mRNA and protein extraction. Paraffin-embedded tumor sections from 259 PSCC patients were re-analyzed by two independent pathologists (CCB and LLL), and immunohistochemistry (IHC) staining was performed.

Target gene screening for the progression of PSCC

Quality-approved paired samples from 8 pN + PSCC patients (including adjacent normal [N], primary carcinoma [PCA] and metastatic lymph node tissues [LM]) were subjected to next-generation CGP with Affymetrix Microarrays (Shanghai Genechem Co., Ltd.) [19]. We defined differentially expressed genes as the absolute value of fold change (FC) ≥ 2 according to the Benjamini–Hochberg method [20]. We further

screened for target genes that were consistently overexpressed in the LM and PCA groups, in particular those higher in the LM group (FC: LM ≥ PCA and PCA:N ≥ 2.5; $p < 0.05$, and FDR < 0.05). Then, we combined the baseline expression level of target genes in PSCC tissues and those revealed in previous reports to identify potential oncogenes for subsequent studies.

Cell lines, culture conditions and transfection methods

Five PSCC cell lines, Penl1, Penl2, 149rca, 149rm and 156lm, were established in our laboratory as previous reported [18]. The normal control human epidermis keratinocyte (HaCaT) cell line was purchased from the Type Culture Collection of the Chinese Academy of Sciences (Shanghai, China). All cell lines were cultured in Dulbecco's modified Eagle's (DMEM) medium with 10% fetal bovine serum (FBS, Gibco). To knock down the expression of target genes, PSCC cell lines were transfected with RNA interference plasmids (GV248; hU6-MCS-Ubiquitin-EGFP-IRES-puromycin; Shanghai Genechem Co., Ltd.) or small interfering RNA (siRNA). The effective short hairpin RNA (shRNA) sequences were as follows: RAB20-sh1, ATCCTCACCTATGATGTGAAT; RAB20-sh2, AAGGAAGAGTGCAGTCCCAAT and shNC, TTCTCCGAACGTGTCACGT. The siRNA sequence GCAACAGTATTTCGGTATAAT was used to knock down the expression of CHK1.

Gene-set Enrichment Analysis (GSEA)

Penl2 PSCC cells were transfected with shRNA (shRAB20 and shNC) to knock down the expression of RAB20, and RNA sequencing (RNA-seq) gene expression analysis was performed. Then, GSEA was conducted on normalized RNA-seq data (shRAB20 *vs.* shNC) by GSEA tools version 4.1 (http://www.broadinstitute.org/gsea*).* We analyzed the subsets of the *Molecular Signatures Database* (C2 and C5) related to cell cycle and cell proliferation and calculated the normalized enrichment score (NES) and the corresponding p-value of the false discovery rate (FDR).

Immunohistochemistry assay

In brief, 4 μm paraffin-embedded tissue sections from 259 PSCC patients were deparaffinized in xylene and rehydrated with an alcohol gradient. Antigens were restored by incubating in citrate buffer, adjusting the pH to 6, and heating for 15 min. Nonspecific antigens were blocked with QuickBlock™ Blocking Buffer (Beyotime) for 15 min. Afterward, sections were incubated with RAB20 antibody (Abcam, ab197209, 1:1000) overnight at 4°C, followed by a 2 h incubation with horseradish peroxidase (HRP)-labeled goat anti-rabbit secondary antibody (Beyotime). Finally, immunochemical staining was visualized by a peroxidase EnVision Detection Kit (Dako). Gene expression was judged independently by two pathologists (Keming Chen and Lilin Liu) blind to the sample identities. The cutoff value was determined by X-Tile software (Version 3.6.1) [21].

Western blot (WB)

Proteins were extracted by RIPA lysis buffer (Beyotime) with 1% phosphatase and protease inhibitors and separated by 10% SDS-PAGE (EpiZyme). Then, we transferred the proteins onto PVDF membranes (Pierce Biotechnology) and blocked them with 5% milk at 37°C for 1 h. The membranes were incubated with

primary antibody overnight at 4°C. A subsequent 2 h incubation in secondary antibody was performed, and the membranes were then exposed to ECL reagents (Abcam). Antibodies and dilutions were as follows: RAB20 antibody (Abcam, ab197209, 1:1000); α-tubulin (CST, #2144, 1:1000); β-actin (CST, #3700, 1:1000); CDK2 (CST, #2546, 1:1000); CyclinE1 (CST, #20808, 1:1000); CyclinD1 (CST, #55506, 1:1000); CyclinB1 (CST, #12231, 1:1000); cdc2 (CST, #9116, 1:1000); Phospho-cdc2 (CST, #4539, 1:1000); Chk1 (CST, #2360, 1:1000); cdc25C (CST, #4688, 1:1000); Phospho-cdc25C (CST, #4901, 1:1000); p53 (CST, #2527, 1:1000); Phospho-p53 (CST, #9286, 1:1000); and p21Waf1/Cip1 (CST, #2947, 1:1000).

Quantitative real-time polymerase chain reaction (qPCR) assay

The extraction (HiPure Total RNA Plus Micro Kit, Magen), reverse transcription (HiScript Q RT SuperMix Kit, Vazyme), and amplification (ChamQ SYBR qPCR Green Master Mix Kit, Vazyme) of mRNA were performed according to the manufacturer's directions. The relative mRNA expression levels of the target genes were calculated by the $2^{(-\Delta\Delta Cq)}$ method and normalized against the expression level of GAPDH. The primers used for the corresponding genes were as follows: GAPDH forward 5'-TGGTGAAGACGCCAGTGGA-3' and reverse 5'-GCACCGTCAAGGCTGAGAAC-3'; RAB20 forward 5'-CTATGATGTGAATCACCGGCAG-3' and RAB20 reverse 5'-GGTCCCCAGCGTCCATATTG-3'.

Cell proliferation, migration, colony formation and wound healing assays

A CCK-8 assay was conducted to explore the proliferation potential of RAB20 cells. A total of 2×10^3 PSCC cells (shRAB20 and negative control [NC]) were seeded into 96-well plates in 100 μl DMEM, incubated with 10 μl CCK-8 solution (Dojindo, Japan) for 2 h, and counted by a microplate reader (optical density: 450 nm) for 7 consecutive days. For the cell migration assay, 10^5 PSCC cells were seeded in the upper compartment of 24-well Transwell chambers in serum-free DMEM, with 10% FBS-DMEM in the lower compartment. The number of migrating cells was counted after a 24 h incubation. For the colony formation assay, 2000 cells were cultured in 6-well plates for 14 days, and the cell colonies were counted by ImageJ (National Institutes of Health, USA). For the wound healing assay, when PSCC cells covered the 6-well plates, cross lines were drawn with 1000 μl pipette tips. After incubation with serum-free DMEM for 16 h, the wound-healing capacity was determined by measuring the size of the gaps.

Cell cycle assay

For cell cycle profiling, Penl2 and 149rca PSCC cells (shRAB20 and shNC groups) were synchronized for 24 h in serum-free DMEM, followed by fixation in 70% ethanol overnight. Then, tumor cells (10^5 per tube) were stained with the Cell Cycle Staining Kit (KeyGEN) according to the manufacturer's instructions. Flow cytometry (ACEA NovoCyte™) was used to explore the percentage of cells in each cell cycle phase and the data were analyzed by NovoExpress™. Cell cycle distribution is presented as histograms from three independent experiments.

Xenograft assay

Five- to seven-week-old male BALB/c nude mice (Jiangsu GemPharmatech Co., Ltd.) were randomly divided into the shRAB20 and NC groups (n = 7) and housed under the same conditions. Each mouse was injected subcutaneously with tumor cells (10^6 Penl2 cells transfected with shRAB20 or shNC in 150 μl phosphate buffer saline) and sacrificed three weeks later. In addition, mice were euthanized when weight loss over 15% or a tumor size exceeding 1500 mm^3 occurred.

Results

The expression profiles of mRNAs in PSCC tissues

To investigate the different profiles of mRNA expression as PSCC progresses, we compared eight pairs of PSCC tissues (including adjacent normal [N], primary carcinoma [PCA] and metastatic lymph node tissues [LM]) by using a comprehensive transcriptome microarray (Table S1). The expression levels of 19 mRNAs were found to be upregulated in both the PCA group and the LM group; mRNA expression upregulation was highest in the LM group, as shown in Fig. 1a and b. Among the 19 genes, we found that the overexpression of RAB20 was correlated with poor PSCC patient prognosis. Thus, RAB20 was further explored in this study.

RAB20 is overexpressed in PSCC cell lines and tissues

To evaluate the expression level of RAB20 in PSCC cells and tissues, WB and IHC were performed to detect the expression of RAB20 protein. Compared with that in normal epithelial cells or tissues, RAB20 protein was overexpressed in five PSCC cell lines and tumor tissues (Fig. 1c and d). The IHC results indicated that RAB20 staining in representative samples of PSCC was preferentially localized in the cytoplasm and was more abundant in tumor tissues than in normal controls (Fig. 1e).

Subsequently, we aimed to validate the mRNA expression of RAB20 in a larger cohort of 78 PSCC patients (15 pairs). Compared with that in 21 normal tissues, RAB20 expression was upregulated in 78 tumor tissues ($t = 3.023$, $p = 0.009$) (Fig. 1f). Further analysis of 15 paired samples showed that the mRNA expression of RAB20 was higher in tumors than in corresponding control tissues, consistent with the WB results ($t = 3.779$, $p < 0.001$) (Fig. 1g).

Overexpression of RAB20 was associated with poor clinical features in PSCC

To identify the association between RAB20 expression and clinical significance, 259 paraffin-embedded PSCC sections were subjected to IHC assays, and the staining patterns are shown in Fig. 1h. High RAB20 expression was regarded as a tumor cytoplasmic staining score > 4, as calculated by X-tile software (Fig. S2). In this cohort, a total of 100 patients (38.6%) died from PSCC, with a median follow-up time of 81.0 months (IQR: 46.0–134.0). The IHC results showed that 147/259 (56.8%) PSCC patients had high RAB20 expression, while 142 (43.2%) patients had low RAB20 expression (Table 1). Chi-square analysis demonstrated that overexpression of RAB20 was positively associated with increased pT and pN status,

metastasis, extranodal extension (ENE) and clinical stage (both $p < 0.01$), indicating poor PSCC patient prognosis (Table 1).

Table 1
Association of RAB20 expression with clinicopathological features of 259 PSCC patients.

		RAB20 IHC staining			
Variable	**PSCC cohort (N = 259), %**	**Low expression (N = 112), %**	**High expression (N = 147), %**	**χ^2**	**p-value [a]**
Age				0.424	0.515
< 55	149 (57.5)	67 (25.9)	82 (31.7)		
≥ 55	110 (42.5)	45 (17.4)	65 (25.1)		
pT status				**17.137**	**0.002[b]**
≤pT1[c]	94 (36.3)	56 (21.6)	38 (14.7)		
pT2	35 (13.5)	13 (5.0)	22 (8.5)		
pT3	96 (37.1)	34 (13.1)	62 (23.9)		
pT4	11 (4.2)	2 (0.8)	9 (3.5)		
Tx	23 (8.9)	7 (2.7)	16 (6.2)		
pN status				**35.484**	**0.000**
N0	123 (47.5)	75 (29.0)	48 (18.5)		
N1	32 (12.4)	11 (4.2)	21 (8.1)		
N2	32 (12.4)	13 (5.0)	19 (7.3)		
N3	72 (27.8)	13 (5.0)	59 (22.8)		
Metastasis				**8.679**	**0.003[b]**
M0	244 (94.2)	111 (42.9)	133 (51.4)		
M1	15 (5.8)	1 (0.4)	14 (5.4)		
Clinical stage[d]				**39.060**	**0.000**
Stage □	65 (25.1)	46 (17.8)	19 (7.3)		
Stage □	57 (22.0)	29 (11.2)	28 (10.8)		
Stage □	56 (21.6)	20 (7.7)	36 (13.9)		
Stage □	81 (31.3)	17 (6.6)	64 (24.7)		

[a]Chi-square test; [b]Fisher's exact test; [c]Included Ta, Tis and pT1 patients; [d]Clinical stage was based on the AJCC Cancer Staging Manual and TNM Staging System for Penile Cancer (8th ed., 2017); ENE, extranodal extension; PSCC, penile squamous cell carcinoma.

		RAB20 IHC staining			
Histology				3.322	0.190
G1	133 (51.4)	63 (24.3)	70 (27.0)		
G2	90 (34.7)	38 (14.7)	52 (20.1)		
G3	36 (13.9)	11 (4.2)	25 (9.7)		
ENE				**19.743**	**0.000**
No	199 (76.8)	101 (39.0)	98 (37.8)		
Yes	60 (23.2)	11 (4.2)	49 (18.9)		

[a]Chi-square test; [b]Fisher's exact test; [c]Included Ta, Tis and pT1 patients; [d]Clinical stage was based on the AJCC Cancer Staging Manual and TNM Staging System for Penile Cancer (8th ed., 2017); ENE, extranodal extension; PSCC, penile squamous cell carcinoma.

Then, survival analyses showed that RAB20 overexpression led to poor CSS outcomes ($p < 0.001$) (Fig. 2a), and consistent results were found in the pT2-pT4, pN+, ENE and pathological grade subgroups (both $p < 0.05$) (Fig. 2b-f). Other clinical features, including pT2-pT4 subgroup, pN status, pathological grade subgroup, ENE were also related to CSS (both $p < 0.05$, Fig. S2). Furthermore, the multivariate analysis demonstrated that RAB20 expression ($p = 0.011$, HR = 2.090; 95% CI: 1.183–4.692) is an independent prognostic factor for poor PSCC patient CSS outcomes (Table 2). These findings suggest that the overexpression of RAB20 is a novel marker associated with poor PSCC clinical features.

Table 2. Univariate and multivariate analyses of clinical and pathological features in 259 PSCC patients.

		Univariate analysis[a]			Multivariate analysis[b]	
Variable	Total N	Events (%)	5-year CSS rate (95% CI)	p-value	Hazard ratio (95% CI)	p-value
Age				**0.037**		0.271
<55	149	51 (34.2)	0.665 (0.583–0.747)		Reference	
≥55	110	49 (44.5)	0.542 (0.442–0.642)		1.304 (0.813–2.091)	
pT status[c]				**0.000**		**0.039**
≤pT1	94	18 (19.1)	0.829 (0.747–0.911)	Reference	Reference	-
pT2	35	15 (42.9)	0.539 (0.365–0.713)	**0.001**	2.135 (1.027–4.438)	**0.042**
pT3	96	41 (42.7)	0.589 (0.483–0.695)	**0.000**	1.970 (1.101–3.526)	**0.022**
pT4	11	10 (90.9)	0.000	**0.000**	3.307 (1.290–8.479)	**0.013**
Histology				**0.000**		0.109
G1	133	37 (27.8)	0.746 (0.670–0.822)	Reference	Reference	-
G2	90	35 (38.9)	0.550 (0.428–0.672)	**0.010**	1.005 (0.567–1.781)	0.986
G3	36	28 (77.8)	0.248 (0.097–0.399)	**0.000**	1.766 (0.936–3.332)	0.079
pN status				**0.000**		**0.000**
N0	123	13 (10.6)	0.910 (0.853–0.967)	Reference	Reference	-
N1	32	11 (34.4)	0.664 (0.492–0.836)	**0.000**	2.135 (1.027–4.438)	**0.005**
N2	32	16 (50.0)	0.481 (0.289–0.673)	**0.000**	1.970 (1.101–3.526)	**0.000**
N3	72	60 (83.3)	0.112 (0.020–0.204)	**0.000**	3.307 (1.290–8.479)	**0.000**
Metastasis				**0.000**		**0.008**
M0	244	85 (34.8)	0.655 (0.590–0.720)		Reference	

M1	15	15 (100)	0.000		2.686 (1.291–5.588)	
Clinical stage[d]				**0.000**		
Stage Ⅰ	65	7 (10.8)	0.900 (0.816–0.984)	Reference	Excluded[e]	
Stage Ⅱ	57	5 (8.8)	0.942 (0.879–1.000)	0.776		
Stage Ⅲ	56	21 (37.5)	0.636 (0.499–0.773)	**0.000**		
Stage Ⅳ	81	67 (82.7)	0.104 (0.020–0.188)	**0.000**		
ENE				**0.000**		0.109
No	199	52 (26.1)	0.754 (0.689–0.819)		Reference	
Yes	60	48 (80.0)	0.116 (0.008–0.224)		1.293 (0.600–2.786)	
RAB20				**0.000**		**0.011**
Low expression	112	21 (18.7)	0.819 (0.739–0.899)		Reference	
High expression	147	79 (53.7)	0.467 (0.383–0.551)		2.090 (1.183–4.692)	

[a]Log-rank test, [b]Cox regression model (Tx patients excluded, n=236), [c]23 Tx patients were excluded and stratified analysis found there was no significant difference between pT2/pT3 (χ^2=0.005, p=0.944), [d]Stratified analysis revealed no significant difference between stage I/stage II (χ^2=0.081, p=0.776), [e]Clincial stage was excluded from the Cox regression model as it was represented by the TNM stage. CSS, cancer-specific survival.

RAB20 promotes cell proliferation and cell cycle progression in PSCC

To investigate the oncogenic function of RAB20, we first suppressed the expression of RAB20 by short hairpin RNAs (shRNAs) in PSCC cell lines (Penl2 and 149rca), and the knockdown efficiency was measured by WB (Fig. 3a). CCK-8 cell proliferation and colony formation assays demonstrated that RAB20-silenced Penl2 and 149rca cells demonstrated dramatically impaired cell growth compared with that of negative controls (Fig. 3b-c). Knockdown of RAB20 inhibited the migration of PSCC cells, as shown in Fig. 3d. Additionally, *in vivo* experiments demonstrated that knockdown of the expression of RAB20 in Penl2 cells resulted in smaller and lighter tumors in BALB/c nude mice (Fig. 3e).

Knockdown of RAB20 induced G2/M cell arrest in PSCC

GSEA was utilized to dissect the molecular mechanisms underlying the role of RAB20 in the progression of PSCC by exploring the gene expression differences between RAB20-silenced Penl2 cells and negative control cells. The results showed significant enrichment in the cell replication and cell cycle checkpoint pathways, indicating a prominent role for RAB20 in cell proliferation (Fig. 3f).

Flow cytometry assays were performed to further investigate the role of RAB20 in the cell cycle. The results showed that the proportion of cells in the G2 phase was dramatically increased from 10.67–26.18% in Penl2 cells and from 16.15–27.30% in 149rca cells when RAB20 was inhibited (Fig. 4a). WB verified that the expression of the critical G2/M regulatory proteins cyclinB1 and cdc2 [22] was significantly downregulated after knockdown of RAB20 in Penl2 and 149rca cells. In contrast, the expression levels of G1/S cell cycle regulators, such as cyclin D1 and the CDK2-cyclin E1 complex [22], were not significantly altered (Fig. 4b). These findings indicate that RAB20 silencing induces G2/M cell arrest in PSCC cells, which contributes to the resulting inhibition of cell proliferation.

RAB20 regulates the cell cycle via the Chk1/cdc25c/cdc2-cyclinB1 *pathway in PSCC*

Recently reported evidence suggests that the Chk1/cdc25c-dependent and Chk2/p53-dependent molecular pathways contribute to the G2/M transition [23–25]. Therefore, we first measured cdc25c and p53 phosphorylation levels by WB. The results revealed that knockdown of RAB20 in PSCC cells increased the expression of Chk1, which promoted the phosphorylation of cdc25c at Ser216 and did not affect total cdc25c protein expression levels [24, 26]. In addition, the phosphorylation levels of p53 and its downstream protein p21 were not affected (Fig. 4c-d). Previous studies demonstrated that the downstream cdc25c phosphatase is responsible for dephosphorylating p-cdc2 and activating the cdc2-cyclinB1 complex, triggering mitosis [26–28]. Consistent with these findings, we found that the ratio of nonphosphorylated cdc25c was reduced in RAB20-silenced PSCC cells, inhibiting the formation of the cdc2-cyclinB1 complex involved in Chk1/cdc25c-mediated G2/M cell cycle arrest (Fig. 4c).

To further validate the potential RAB20-mediated Chk1/cdc25c/cdc2-cyclinB1 pathway in G2/M cell cycle arrest, we performed rescue experiments by repressing Chk1 expression in shRAB20 PSCC cells. Figure 4e shows that the percentage of RAB20-silenced Penl2 and 149rca cells transfected with Chk1-siRNA in G2 phase decreased from 23.08–7.63% and 24.74–5.42%, respectively (Fig. 4e), indicating that RAB20-mediated G2/M cell cycle arrest was Chk1/cdc25c-dependent. Moreover, the phosphorylation of cdc25c and cdc2 was inhibited in RAB20-silenced PSCC cells transfected with siChk1, whereas the protein levels of cdc2-cyclinB1 were elevated (Fig. 4f). Taken together, our results demonstrate that knockdown of RAB20 represses cell proliferation at the G2/M phase via the Chk1/cdc25c/cdc2-cyclinB1 pathway in PSCC.

Discussion

PSCC is more common in developing countries, such as China, than in the United States and Europe. Chinese PSCC patients account for 1/3 of new cases worldwide and PSCC is substantial health concern due to its mental and physical effects [29, 30]. Although the TNM staging system, especially the pT stage, is a convenient and effective clinical prognostic tool for evaluating survival, the ability to perform precise and individualized assessment with this approach is limited by tumor heterogeneity [7, 8, 31]. Recently, several sequencing studies in Europe and the Americas have revealed the clinically relevant genomic alterations in PSCC and provided a better understanding of tumor progression and targets for therapy [7–11]. However, potential prognostic biomarkers and specific mechanisms of action remain unknown due to the lack of experimental data and large-cohort clinical validation; in particular, analysis of the genomic expression pattern in Chinese PSCC patients had not been previously reported [7–11]. Therefore, for the first time, we performed whole-transcriptome microarray profiling of paired PSCC tissues to explore the genomic landscape in Chinese patients and to investigate the potential biomarkers and mechanisms of PSCC.

In this study, we found that the expression of RAB20, a small GTPase family member located on chromosome 13q34 [32], was upregulated in PSCC matched tumor tissues, especially in metastatic lymph nodes. qPCR, WB and IHC further confirmed that RAB20 was overexpressed in the cytoplasm of five PSCC cell lines and 78 PSCC tumor tissues compared with that in the corresponding normal controls. The results highlight that RAB20 might be a crucial oncogene participating in the development and progression of PSCC, although the roles of RAB20 in PSCC have not yet been reported.

Recent studies have revealed that RAB20, which plays a role in the control of endocytotic vesicle transport, is involved in the progression of multiple cancers [15–17, 33]. Amillet et al. [15] first identified that the overexpression of RAB20 in pancreatic intraductal neoplasia lesions is an early event in the course of pancreatic cancer progression [15]. Habermann et al. [17] demonstrated that RAB20 overexpression and amplification indicated genomic instability in colorectal adenomas and was correlated with high-grade histopathological features and tumor recurrence [17]. In addition, the overexpression of RAB20 in triple-negative breast cancer has been associated with advanced disease stage and poor patient prognosis [16].

To further explore the clinical significance of RAB20 expression in PSCC, correlation and survival analyses were conducted on 259 PSCC patients, the largest cohort reported to date, with a median follow-up time of over six years. The overexpression of RAB20 in PSCC was positively associated with advanced clinicopathological features and a shorter 5-year CSS time. Moreover, RAB20 was found to be a strong independent prognostic indicator of poor clinical outcomes, identifying PSCC patients with an increased risk for tumor progression and a shorter survival time. These findings underscore the clinical significance of RAB20 in PSCC and imply that RAB20 plays oncogenic roles in tumor progression.

A recent study on neuronal network formation showed that RAB20, as a novel regulator, participated in neurite outgrowth and cell proliferation [34]. Liu et al. [33] found that the restoration of RAB20 expression

in hepatocellular carcinoma cells inhibited cell growth, motility and metastasis. To further investigate the oncogenic functions of RAB20 in regulating the malignant phenotype, validation experiments were conducted *in vitro* and *in vivo.* We observed that knockdown of RAB20 in our newly established PSCC cell lines repressed colony formation, cell proliferation, and migration along with repressing tumor growth in xenografted nude mice. Interestingly, GSEA showed that RAB20-silenced Penl2 cells were not only enriched in cell proliferation pathways but also in cell cycle checkpoint pathways. Habermann et al. [17] reported that RAB20 amplification triggered EGFR recycling and promoted cell proliferation by increasing the formation of cyclin A-CDK2 complexes in the S/G2 cell cycle phases [17]. Therefore, we explored the cell cycle distribution by flow cytometry, and the results indicated that RAB20-silenced PSCC cells exhibited G2/M phase cell cycle arrest but unaffected G1/S transition. Similarly, knockdown of RAB20 did not inhibit the expression of the CDK2-cyclinE1 complex, the key effector in the G1/S phase, but significantly suppressed cdc2-cyclinB1 levels at the G2/M transition [22]. Overall, we found that RAB20-mediated cancer progression could be tumor-type specific and promotes PSCC proliferation by regulating G2/M cell cycle checkpoints.

Cdc25c phosphatase promotes the mitotic cell G2/M transition by triggering cdc2 dephosphorylation to activate the cdc2-cyclinB1 complex [26, 28]. The activation of cdc25c requires phosphorylation within the N-terminal domain at Thr48, Thr67, Ser122, Thr130 or Ser216 sites, which is regulated by the checkpoint protein kinases Chk1 and Chk2 and p53 pathways [28]. We found that knockdown of RAB20 did not alter the phosphorylation of p53 or the transcriptional activation of p21 (a downstream protein in the p53 pathway) [23]. However, in shRAB20 PSCC cells, the Chk1-mediated phosphorylation of cdc25c at Ser216 was increased and the cdc2-cyclinB1 complex was inhibited. Subsequently, we measured the cell cycle stage distribution and protein expression when Chk1 was repressed in shRAB20 PSCC cells. We found a remarkable decrease in the proportion of cells in G2, and the expression levels of the cdc2-cyclinB1 complex and p-cdc25c (Ser216) were restored. The results further demonstrate that RAB20 induces G2/M phase cell arrest via the Chk1/cdc25c pathway in PSCC.

Our study also has some limitations. We focused on the oncogenes that were upregulated in the comprehensive genomic sequencing and did not study the potential tumor suppressor genes that might promote the progression of PSCC. Second, the detailed mechanisms by which RAB20 regulates Chk1 in G2/M cell cycle arrest should be further investigated. Third, more efforts at multiple centers are required to determine the potential value of RAB20 as a biomarker for PSCC.

Conclusions

In the current study, we explored the potent oncogene RAB20, which is overexpressed in PSCC and is associated with advanced clinicopathological features and poor patient prognoses. High RAB20 expression promotes tumor progression and cell proliferation, inducing G2/M cell cycle arrest via the Chk1/cdc25c/cdc2-cyclinB1 pathway. RAB20 could be a potential therapeutic target and serve as a novel prognostic indicator of PSCC patient outcomes.

Abbreviations

CGP: comprehensive genomic profiling, Chk1: checkpoint kinase 1, CI: confidence interval, CSS: cancer-specific survival, CCK-8: cell counting kit-8, DMEM: Dulbecco's Modified Eagle's Medium, ENE: extranodal extension, FBS: fetal bovine serum, FC: fold change, FDR: false discovery rate, GSEA: gene-set enrichment analysis, HaCaT: human immortalized keratinocytes, HR: hazard ratio, IHC: immunohistochemistry, mRNA: messenger RNA, NES: normalized enrichment score, pN+: pathological node-positive, PSCC: penile squamous cell carcinoma, qPCR: quantitative polymerase chain reaction, shRNA: short hairpin RNA, siRNA: small interfering RNA, SYSUCC: Sun Yat-sen University Cancer Center, WB: Western blot.

Declarations

Ethics approval and consent to participate

This study was approved by the *Ethics Committee of SYSUCC* (No. 2020-FXY-056), and informed consent was obtained from all of the PSCC patients (B2020-073). The animal experiments was approved by the *Experimental Animal Ethics Committee of SYSUCC* (L102022021001D).

Consent for publication

All of the authors are agree to the content of the paper and consent to public.

Availability of data and materials

The authenticity of this article has been validated by uploading the key raw data onto the Research Data Deposit platform (www.researchdata.org.cn), with the approval RDD number as RDDB2021956079.

Competing interests

The authors declare no conflicts of interest.

Funding

This study was supported by the Fundamental Research Funds for the Central Universities (No. 19ykpy178 to Kai Yao), the Natural Science Foundation of Guangdong Province (No. 2019A1515010197 to Kai Yao), the Sun Yat-sen University Cancer Center Medical Scientist Training Program (No. 14zxqk08 to Kai Yao) and the Natural Science Foundation of Chongqing (No. cstc2019jcyj-msxmX0420 to Gangjun Yuan).

Authors' contributions

TXL and YGJ were the contributor in writing the manuscript. WYJ and CD were responsible for the sample collection. TXL, ZYT and LSH performed the experiments *in vitro*. HH, QZK conducted the statistical

analysis. LZW was responsible for the animal experiments. ZFJ reviewed the article data. LYL and YK designed the supported the study. All authors read and approved the final manuscript.

Acknowledgements

We appreciate Cunbiao Cu and Lilin Liu for providing pathological assistance.

References

1. Hakenberg OW, Drager DL, Erbersdobler A, Naumann CM, Junemann KP, Protzel C. The diagnosis and treatment of penile cancer. Dtsch Arztebl Int. 2018,115:646-52.
2. Siegel RL, Miller KD, Fuchs HE, Jemal A. Cancer statistics, 2021. CA Cancer J Clin. 2021,71:7-33.
3. Ficarra V, Akduman B, Bouchot O, Palou J, Tobias-Machado M. Prognostic factors in penile cancer. Urology. 2010,76:S66-73.
4. Leone A, Diorio GJ, Pettaway C, Master V, Spiess PE. Contemporary management of patients with penile cancer and lymph node metastasis. Nat Rev Urol. 2017,14:335-47.
5. O'Brien JS, Perera M, Manning T, Bozin M, Cabarkapa S, Chen E, et al. Penile cancer: contemporary lymph node management. J Urol. 2017,197:1387-95.
6. Hu J, Cui Y, Liu P, Zhou X, Ren W, Chen J, et al. Predictors of inguinal lymph node metastasis in penile cancer patients: a meta-analysis of retrospective studies. Cancer Manag Res. 2019,11:6425-41.
7. Busso-Lopes AF, Marchi FA, Kuasne H, Scapulatempo-Neto C, Trindade-Filho JC, de Jesus CM, et al. Genomic profiling of human penile carcinoma predicts worse prognosis and survival. Cancer Prev Res (Phila). 2015,8:149-56.
8. Ali SM, Pal SK, Wang K, Palma NA, Sanford E, Bailey M, et al. Comprehensive genomic profiling of advanced penile carcinoma suggests a high frequency of clinically relevant genomic alterations. Oncologist. 2016,21:33-9.
9. McDaniel AS, Hovelson DH, Cani AK, Liu CJ, Zhai Y, Zhang Y, et al. Genomic profiling of penile squamous cell carcinoma reveals new opportunities for targeted therapy. Cancer Res. 2015,75:5219-27.
10. Jacob JM, Ferry EK, Gay LM, Elvin JA, Vergilio JA, Ramkissoon S, et al. Comparative genomic profiling of refractory and metastatic penile and nonpenile cutaneous squamous cell carcinoma: Implications for selection of systemic therapy. J Urol. 2019,201:541-8.
11. Marchi FA, Martins DC, Barros-Filho MC, Kuasne H, Busso Lopes AF, Brentani H, et al. Multidimensional integrative analysis uncovers driver candidates and biomarkers in penile carcinoma. Sci Rep. 2017,7:6707.
12. Zhou QH, Han H, Lu JB, Liu TY, Huang KB, Deng CZ, et al. Up-regulation of indoleamine 2,3-dioxygenase 1 (IDO1) expression and catalytic activity is associated with immunosuppression and poor prognosis in penile squamous cell carcinoma patients. Cancer Commun (Lond). 2020,40:3-15.

13. Zhou QH, Deng CZ, Chen JP, Huang KB, Liu TY, Yao K, et al. Elevated serum LAMC2 is associated with lymph node metastasis and predicts poor prognosis in penile squamous cell carcinoma. Cancer Manag Res. 2018,10:2983-95.
14. Stenmark H. Rab GTPases as coordinators of vesicle traffic. Nat Rev Mol Cell Biol. 2009,10:513-25.
15. Amillet JM, Ferbus D, Real FX, Antony C, Muleris M, Gress TM, et al. Characterization of human Rab20 overexpressed in exocrine pancreatic carcinoma. Hum Pathol. 2006,37:256-63.
16. Turner N, Lambros MB, Horlings HM, Pearson A, Sharpe R, Natrajan R, et al. Integrative molecular profiling of triple negative breast cancers identifies amplicon drivers and potential therapeutic targets. Oncogene. 2010,29:2013-23.
17. Habermann JK, Brucker CA, Freitag-Wolf S, Heselmeyer-Haddad K, Kruger S, Barenboim L, et al. Genomic instability and oncogene amplifications in colorectal adenomas predict recurrence and synchronous carcinoma. Mod Pathol. 2011,24:542-55.
18. Zhou QH, Deng CZ, Li ZS, Chen JP, Yao K, Huang KB, et al. Molecular characterization and integrative genomic analysis of a panel of newly established penile cancer cell lines. Cell Death Dis. 2018,9:684.
19. Raman T, O'Connor TP, Hackett NR, Wang W, Harvey BG, Attiyeh MA, et al. Quality control in microarray assessment of gene expression in human airway epithelium. BMC Genomics. 2009,10:493.
20. Ritchie ME, Phipson B, Wu D, Hu Y, Law CW, Shi W, et al. limma powers differential expression analyses for RNA-sequencing and microarray studies. Nucleic Acids Res. 2015,43:e47.
21. Camp RL, Dolled-Filhart M, Rimm DL. X-tile: a new bio-informatics tool for biomarker assessment and outcome-based cut-point optimization. Clin Cancer Res. 2004,10:7252-9.
22. Kastan MB, Bartek J. Cell-cycle checkpoints and cancer. Nature. 2004,432:316-23.
23. Taylor WR, Stark GR. Regulation of the G2/M transition by p53. Oncogene. 2001,20:1803-15.
24. Bartek J, Lukas J. Chk1 and Chk2 kinases in checkpoint control and cancer. Cancer Cell. 2003,3:421-9.
25. Löbrich M, Jeggo PA. The impact of a negligent G2/M checkpoint on genomic instability and cancer induction. Nat Rev Cancer. 2007,7:861-9.
26. Bouldin CM, Kimelman D. Cdc25 and the importance of G2 control: insights from developmental biology. Cell Cycle. 2014,13:2165-71.
27. Liao WL, Lin JY, Shieh JC, Yeh HF, Hsieh YH, Cheng YC, et al. Induction of G2/M phase arrest by diosgenin via activation of Chk1 kinase and Cdc25C regulatory pathways to promote apoptosis in human breast cancer cells. Int J Mol Sci. 2019,21:172.
28. Liu K, Zheng M, Lu R, Du J, Zhao Q, Li Z, et al. The role of CDC25C in cell cycle regulation and clinical cancer therapy: a systematic review. Cancer Cell Int. 2020,20:213.
29. Christodoulidou M, Sahdev V, Houssein S, Muneer A. Epidemiology of penile cancer. Curr Probl Cancer. 2015,39:126-36.
30. Pang C, Guan Y, Li H, Chen W, Zhu G. Urologic cancer in China. Jpn J Clin Oncol. 2016,46:497-501.

31. Sali AP, Menon S, Murthy V, Prakash G, Bakshi G, Joshi A, et al. A modified histopathologic staging in penile squamous cell carcinoma predicts nodal metastasis and outcome better than the current AJCC staging. Am J Surg Pathol. 2020,44:1112-7.
32. Stein MP, Dong J, Wandinger-Ness A. Rab proteins and endocytic trafficking: potential targets for therapeutic intervention. Adv Drug Deliv Rev. 2003,55:1421-37.
33. Liu BHM, Tey SK, Mao X, Ma APY, Yeung CLS, Wong SWK, et al. TPI1-reduced extracellular vesicles mediated by Rab20 downregulation promotes aerobic glycolysis to drive hepatocarcinogenesis. J Extracell Vesicles. 2021,10:e12135.
34. Oguchi ME, Etoh K, Fukuda M. Rab20, a novel Rab small GTPase that negatively regulates neurite outgrowth of PC12 cells. Neurosci Lett. 2018,662:324-30.

Figures

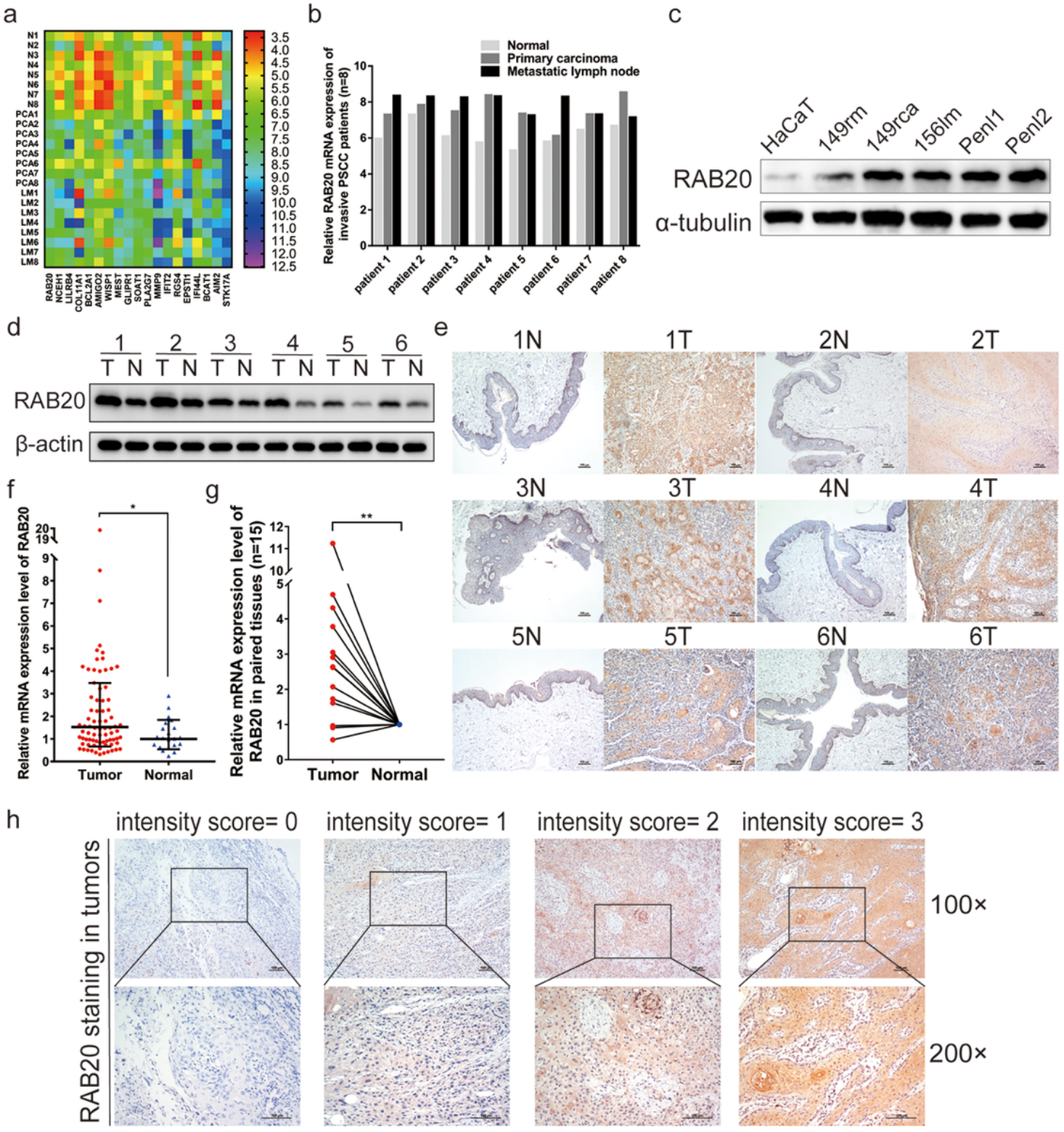

Figure 1

Expression levels of RAB20 in PSCC tissues and cell lines. (a) The comprehensive CGP analysis of eight pN+ PSCC patients indicated 108 co-upregulated genes in the PCA group and LM group, of which 19 genes were more highly expressed in the LM group. The heatmap shows the expression pattern of the 19 target genes. (b) The mRNA expression levels of RAB20 in paired tissues from eight pN+ PSCC patients. (c-d) The RAB20 protein was overexpressed in PSCC cell lines and tumor tissues. (E) IHC staining

indicated that RAB20 was highly expressed in tumors compared with in corresponding normal tissues. (f-g) The mRNA levels of RAB20 were upregulated in 78 tumor tissues compared with those in 21 normal tissues (15 pairs). (h) The expression pattern of RAB20 protein by IHC. The standard staining intensity score of RAB20 in the cytoplasm was 0 for no staining, 1 for weak staining, 2 for clear staining and 3 for strong staining. *p < 0.05, **p < 0.01. HaCaT, human immortalized keratinocytes, IHC, immunohistochemistry.

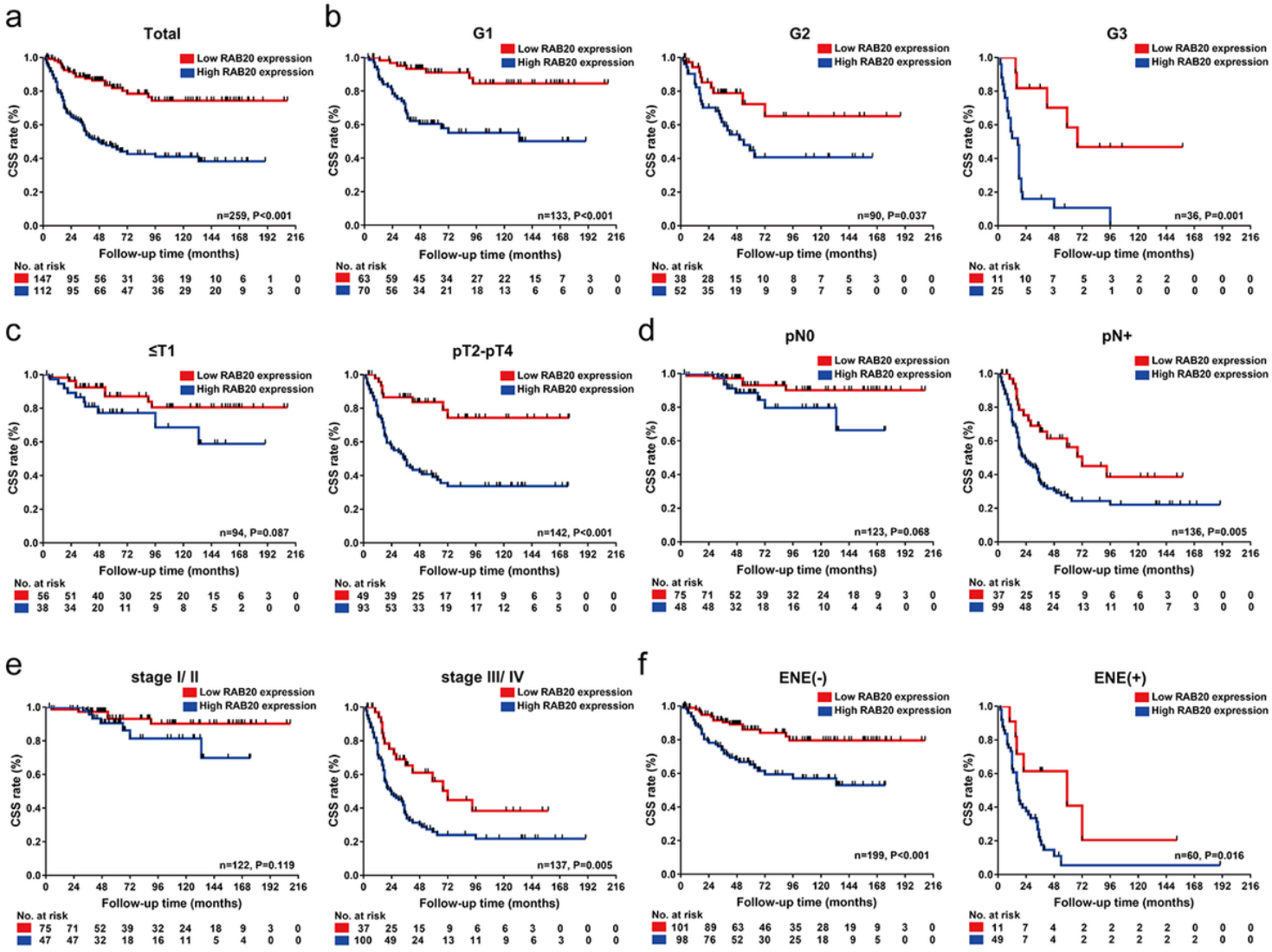

Figure 2

Survival analysis between RAB20 expression and clinical features in 259 PSCC patients. Kaplan–Meier survival analysis was performed to determine the RAB20 expression level in PSCC patients. (a) High RAB20 expression indicated a significantly lower CSS rate in the entire cohort, (b) pathological grade subgroup, (c) pT2-pT4 subgroup, (d) positive lymph node metastasis subgroup, (e) clinical stage III/IV subgroup and (f) ENE subgroup of PSCC patients (p< 0.05). CSS, cancer-specific survival, ENE, extranodal extension.

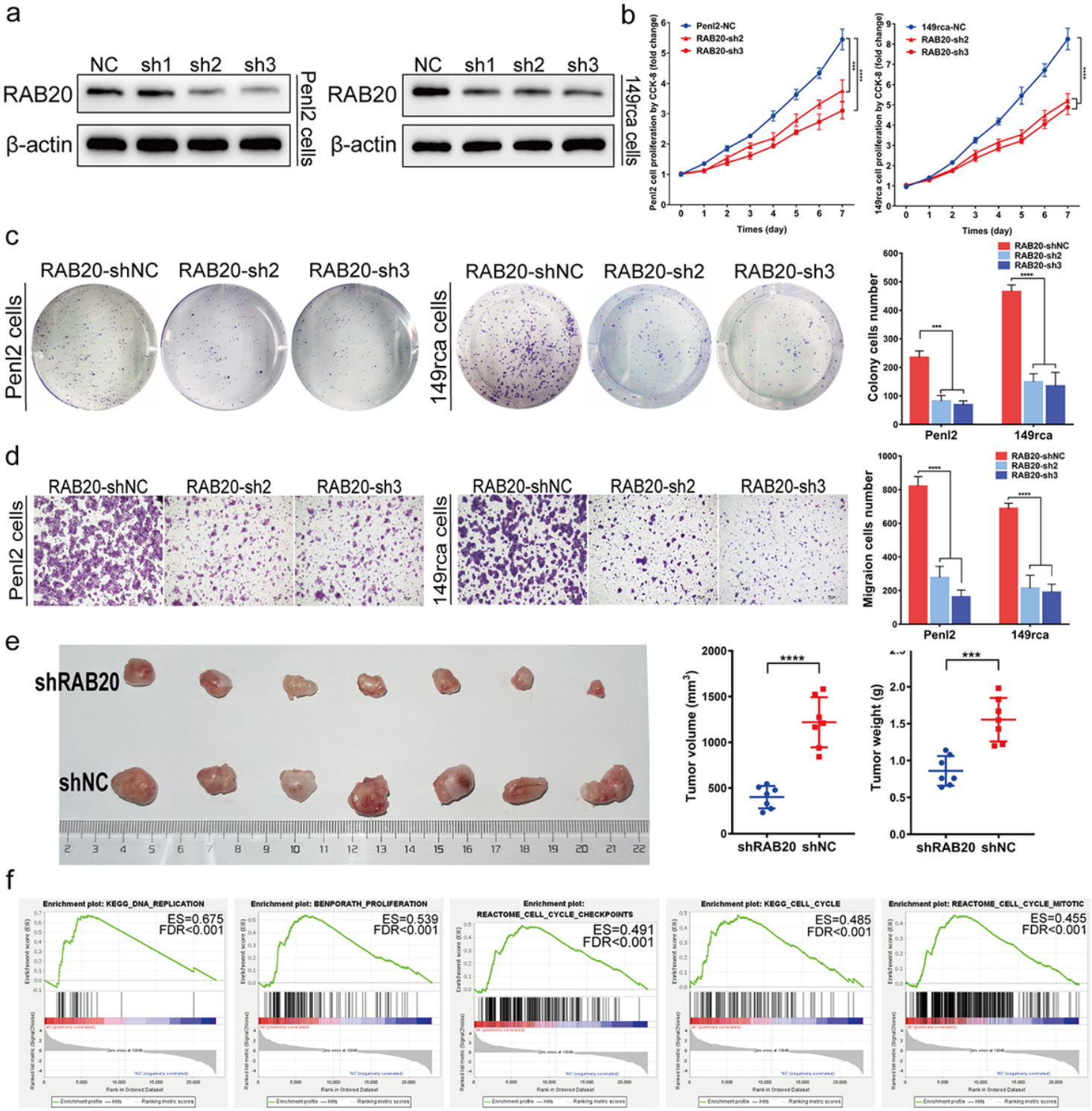

Figure 3

Knockdown of RAB20 inhibited the proliferation of PSCC cells in vivo and in vivo. (a) Western blotting was performed to examine the knockdown efficacy in Penl2 and 149rca RAB20-silenced cells. (b) Knockdown of RAB20 in PSCC cells inhibited cell proliferation, (c) colony formation, (d) cell migration in vitro, (e) and tumor growth in vivo. (f) GSEA showed that knockdown of RAB20 in Penl2 cells significantly influenced the expression of proteins in the cell cycle and proliferation. Statistics are presented as the

means ± SDs of three independent experiments. *p < 0.05, **p < 0.01, ***p < 0.001. GSEA, gene set enrichment analysis, NC, negative control.

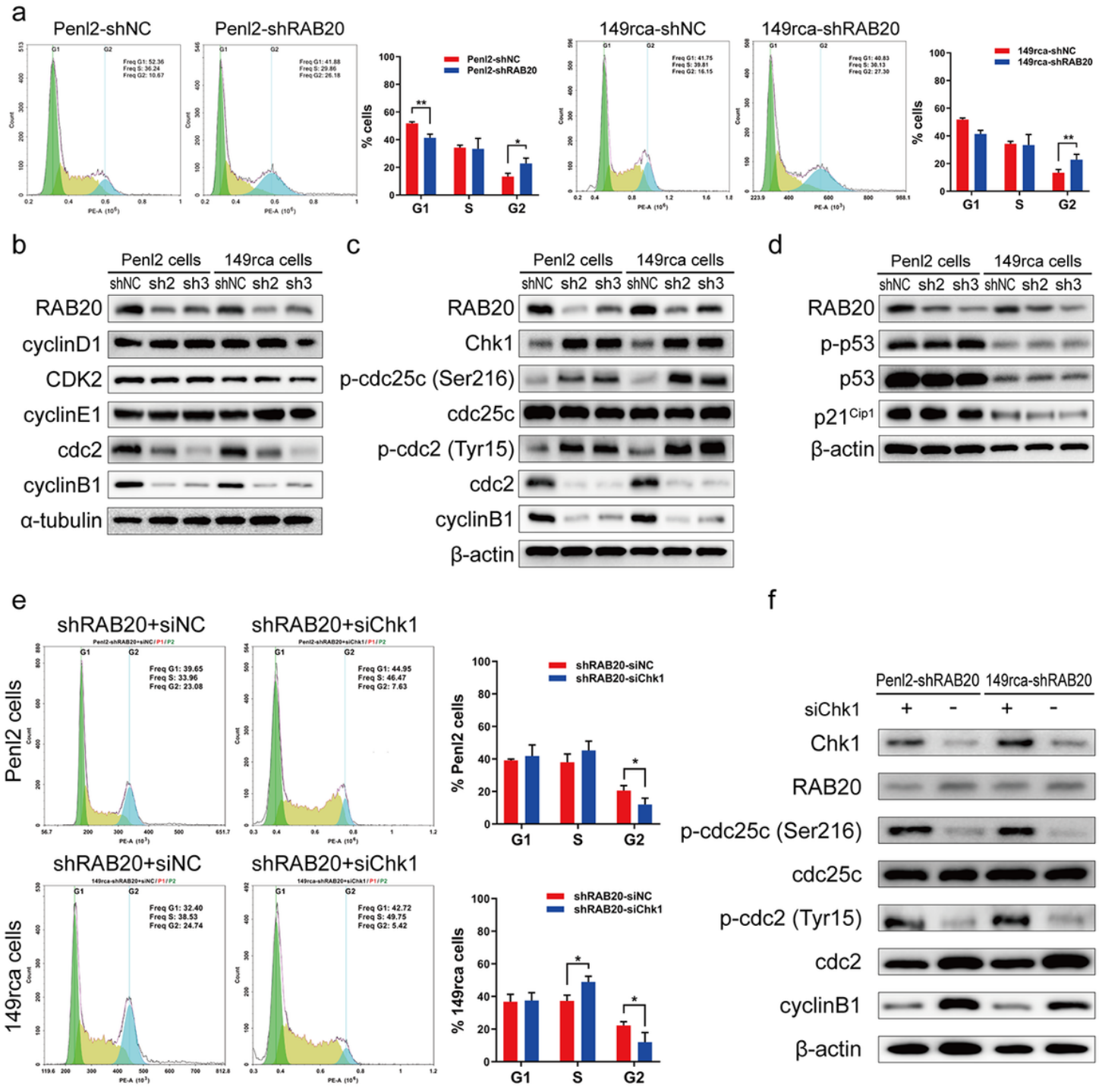

Figure 4

Knockdown of RAB20 induced G2/M cell arrest via the Chk1/cdc25c/cdc2-cyclinB1 pathways. (a) Knockdown of RAB20 increased the proportion of cells in the G2 phase and inhibited cell proliferation. (b) Knockdown of RAB20 significantly reduced the expression of the G2/M checkpoint proteins cdc2 and cyclinB1 but did not influence the G1/S phase. (c, d) Knockdown of RAB20 induced cell cycle arrest at the G2/M phase via the Chk1/cdc25c/cdc2-cyclinB1 pathway rather than via the p53 pathway. (e, f)

Knockdown of Chk1 dramatically attenuated G2/M cell arrest in RAB20-silenced cells and recovered the expression of the G2/M checkpoint proteins cdc2 and cyclinB1. Flow cytometry was performed in triplicate and the results are presented as the mean ± SD. *p < 0.05, **p < 0.01.

Supplementary Files

This is a list of supplementary files associated with this preprint. Click to download.

- SupplementaryFigure1.docx
- SupplementaryFigure2.docx
- SupplementaryTable1.docx